ISSN 1063-7761, Journal of Experimental and Theoretical Physics, 2010, Vol. 111, No. 2, pp. 231–235. © Pleiades Publishing, Inc., 2010.
Original Russian Text © N.B. Gruzdev, V.I. Sokolov, A.E. Ermakov, M.A. Uimin, A.A. Mysik, V.A. Pustovarov, 2010, published in Zhurnal Éksperimental'noĭ i Teoreticheskoĭ Fiziki, 2010, Vol. 138, No. 2, pp. 261–265.

ELECTRONIC PROPERTIES OF SOLID

Excitons and Photoluminescence in ZnO and $Zn_{0.99}Mn_{0.01}O$ Nanocrystals

N. B. Gruzdev[a], V. I. Sokolov[a], A. E. Ermakov[a], M. A. Uimin[a], A. A. Mysik[a], and V. A. Pustovarov[b]

[a] *Institute of Metal Physics, Russian Academy of Sciences, Ural Division, ul. S. Kovalevskoi 18, Yekaterinburg, 620990 Russia*

[b] *Eltsin Ural State Technical University, Yekaterinburg, 620002 Russia*

e-mail: visokolov@imp.uran.ru

Received October 30, 2009

Abstract—The photoluminescence and photoluminescence excitation spectra for $Zn_{1-x}Mn_xO$ nanocrystals are presented. After annealing of powders in air, the intensity of the bands attributable to manganese decreases noticeably. This suggests that the oxygen vacancies affect the Zhang–Rice-like states appearing due to strong *d*–*p*-hybridization, which is confirmed by an increase in the band gap of $Zn_{1-x}Mn_xO$ for low *x*. The origin of the 2.9-eV peak and the shape of its excitation spectrum are discussed qualitatively. For $Zn_{1-x}Mn_xO$ nanocrystals, the shape of the excitation spectrum is as unusual as the intense absorption in the range (2.2–3.0) eV.

DOI: 10.1134/S1063776110080121

$Zn_{1-x}Mn_xO$ semiconductor crystals attract great attention due to the potentiality for creating optoelectronic devices based on a semiconductor with ferromagnetic ordering with a Curie temperature T_C above the room one. In recent years, interest in nanomaterials, including those based on $Zn_{1-x}Mn_xO$, has increased. As a rule, oxide compounds are produced in the form of nanocrystals with a large number of defects (e.g., oxygen vacancies). Analysis of experimental results shows that the oxygen vacancies can play an important role in the formation of magnetic ordering in oxide semiconductors with impurities of 3*d*-elements ZnO:Cr [1] and TiO_2:Co [2] as well as in undoped ZnO [3]. Thus, it seems important to investigate ZnO and $Zn_{1-x}Mn_xO$ nanopowders with sublattice oxygen vacancies by optical methods.

Recently, a 2.9 eV photoluminescence (PL) peak was detected for $Zn_{0.99}Mn_{0.01}O$ nanopowders produced by the gas-phase synthesis method [4]. The excitation spectrum of this emission exhibits three wide peaks in the region of interband transitions at energies of 3.9, 4.5, and 5.3 eV. In this paper, we investigate the $Zn_{0.99}Mn_{0.01}O$ system to understand why the 2.9 eV peak appears in the PL spectrum and the well-studied ZnMnS system for comparison. Our results suggest that a series of states the optical transitions between which and the ground state of the crystal produce both the 2.9 eV peak in the PL spectrum and the features in the excitation spectrum of this emission at energies of 3.9, 4.5, and 5.3 eV in the region of interband transitions emerge in the $Zn_{1-x}Mn_xO$ semiconductor compound.

$Zn_{0.99}Mn_{0.01}O$ nanopowders with a crystal size of 30 nm were produced by the gas-phase synthesis method [5] and were annealed in air at a temperature of 400°C for an hour. The samples for our measurements were produced by tablet pressing at a pressure of 0.5 GPa. The $Zn_{1-x}Mn_xO$ ($x = 0.0016$) single crystals were annealed in air at a temperature of 700°C for 20 hours. The manganese concentration in the nanopowders before and after annealing was measured by inductively coupled plasma mass spectroscopy. The PL and PL excitation (PLE) spectra were measured in the range (2–5.5) eV using two double DMP-4 prism monochromators (a reciprocal linear dispersion of 10 Å mm^{-1} near 5 eV), an R6358-10 (Hamamatsu) photomultiplier tube, and a photon-counting system. A deuterium DDS-400 lamp was used for excitation. The PLE spectra were normalized to the same number of photons incident on the sample using yellow phosphor, which has an energy-independent PL quantum yield in the investigated energy range. The PL spectra are presented without any normalization to the spectral sensitivity of the optical section.

Figure 1 presents the PL and PLE spectra for $Zn_{0.99}Mn_{0.01}O$ nanopowders before and after annealing. In both cases, the PL spectra exhibit low-energy peaks with 2.10 and 2.34 eV maxima and a high-energy peak with a 2.9 eV maximum. The low-energy peaks are attributable to deep defects in the crystals that passed thermal treatment in an oxygen atmosphere [6]. We believe that the number of oxygen vacancies decreased as a result of annealing in air. The weakening of the 2.9 eV peak, which is pronounced in Fig. 1a (curves *2* and *3*), probably stems from the fact

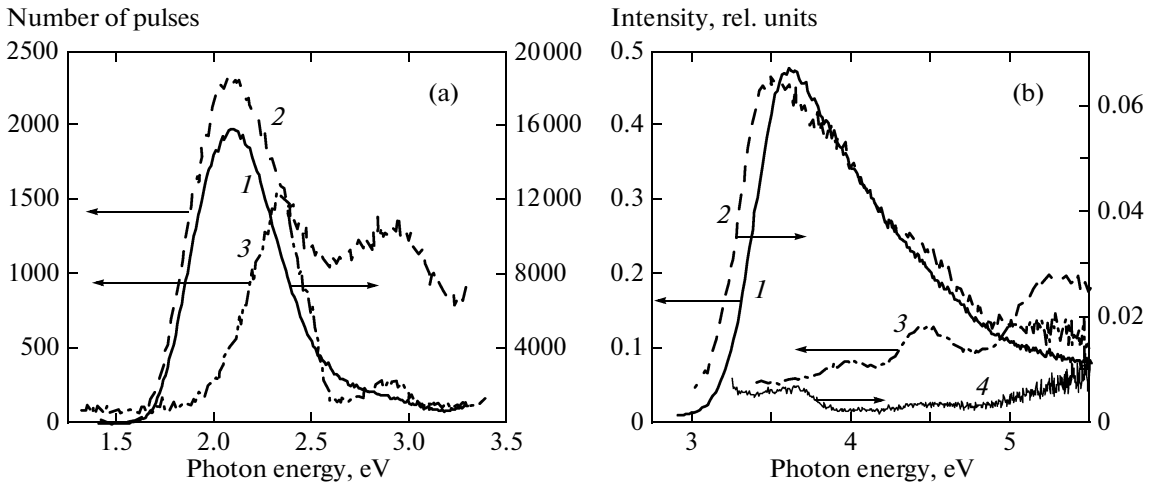

Fig. 1. (a) PL spectra for ZnO (*1*) and $Zn_{0.99}Mn_{0.01}O$ (*2*) nanocrystals before annealing (excitation energy $E = 3.64$ eV, temperature $T = 86$ K) and an annealed $Zn_{0.99}Mn_{0.01}O$ (*3*) nanocrystal (excitation energy $E = 3.718$ eV, temperature $T = 90$ K). (b) PLE spectra of the 2.10-eV peak for ZnO (*1*) and $Zn_{0.99}Mn_{0.01}O$ (*2*) nanocrystals and of the 2.9 eV peak for a $Zn_{0.99}Mn_{0.01}O$ nanocrystal before annealing (*3*) ($T = 86$ K) and after annealing (*4*) ($T = 90$ K, excitation energy $E = 3.89$ eV).

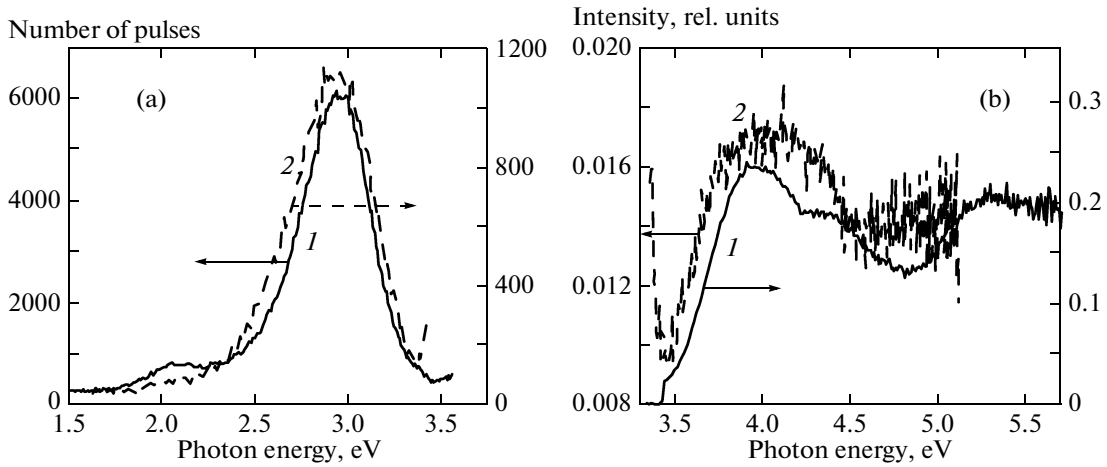

Fig. 2. (a) PL spectra for a ZnO:Mn single crystal (0.16 at.%) before annealing (*1*) (excitation energy $E = 3.84$ eV, temperature $T = 80$ K) and an annealed ZnO:Mn single crystal (*2*) (excitation energy $E = 3.85$ eV, temperature $T = 300$ K). (b) Excitation spectrum of the 2.9 eV peak for a ZnO:Mn single crystal before annealing (*1*) ($T = 80$ K) and after annealing of ZnO:Mn (*2*) ($T = 300$ K).

that this peak is produced by the Mn^{2+} + close environment complex, including the oxygen vacancy V_O. An increase in the intensity with distinct peaks V_1, V_2, and V_3 at energies of 3.9, 4.5, and 5.3 eV is observed in the excitation spectrum of the 2.9 eV peak for an unannealed powder [4]. After annealing, the PL yield decreases, but the increase in the intensity of the PLE spectrum with increasing photon energy is pronounced.

Figure 2 presents the PL and PLE spectra for a ZnO:Mn single crystal before and after annealing in air. The peak in the PL spectrum with an energy of 2.9 eV after annealing decreases noticeably, while the PLE spectrum has a maximum near 4 eV and retains a clear tendency to increase near 5 eV.

For comparison, we provide the PL and PLE spectra for a $Zn_{0.995}Mn_{0.005}S$ single crystal (Fig. 3). The emission with an energy of 2.12 eV is attributable to intracenter Mn^{2+} transitions ($^4T_1$–$^6A_1$), while the PLE spectrum contains the peaks due to the transitions to high-energy Mn^{2+} states ($^4T_2$ and $^4A_2$, ^4E) and a maximum near E_g and a gradual decrease in the intensity at $\hbar\omega > E_g$ are observed in the region of interband transitions. A similar decrease in the excitation intensity at $\hbar\omega > E_g$ manifests itself for the 2.10-eV emission peak in $Zn_{0.99}Mn_{0.01}O$ nanopowders [4] attributable to the

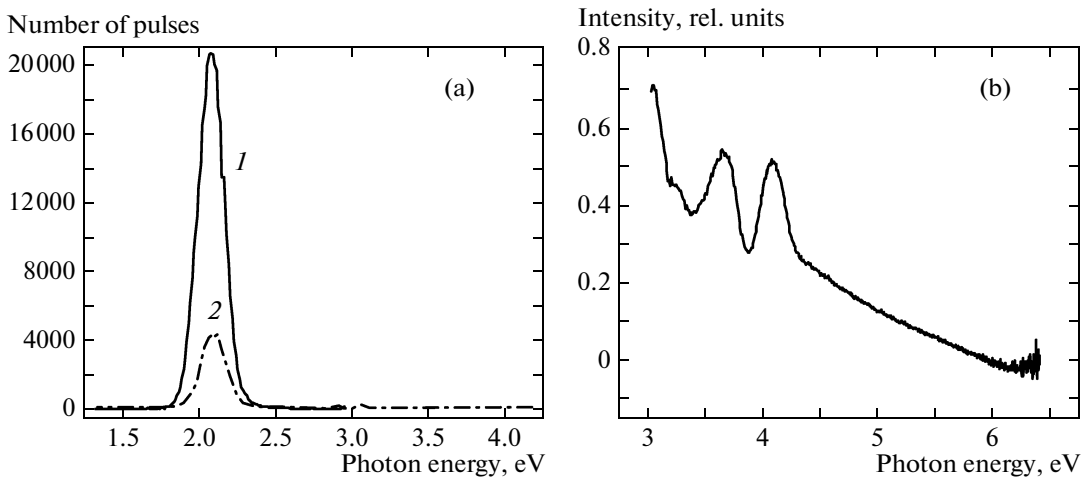

Fig. 3. (a) PL spectra for $Zn_{1-x}Mn_xS$ ($x = 0.55\%$) single crystals. The excitation energy $E = 3.230$ (*1*) and 4.782 (*2*) eV, $T = 300$ K. (b) Excitation spectrum of the 2.12-eV peak for a $Zn_{1-x}Mn_xS$ ($x = 0.55\%$) single crystal, $T = 300$ K.

transitions via deep states (these spectra are also presented in Fig. 1b for comparison).

We see that the excitation spectrum of the 2.9-eV emission for $Zn_{0.99}Mn_{0.01}O$ nanopowders differs significantly both from the excitation spectrum of the 2.10 eV emission for the same $Zn_{0.99}Mn_{0.01}O$ nanopowders via deep levels and from the excitation spectrum of the 2.12 eV emission for the $Zn_{0.995}Mn_{0.005}S$ single crystal via intracenter Mn^{2+} transitions ($^4T_1$–$^6A_1$). In the latter cases, the PL level decreases at $\hbar\omega > E_g$, because the absorption coefficient increases in the region of fundamental absorption. As a result, the depth of the layer that absorbs the exciting photons decreases and charge carriers emerge on the surface, where nonradiative annihilation exceeds radiative recombination due to enhanced imperfection.

The increase in the intensity of the excitation spectrum with increasing $\hbar\omega$ in the region of interband transitions is quite unusual for semiconductor materials. The cause of the increase in the intensity of the 2.9 eV peak for $Zn_{0.99}Mn_{0.01}O$ at $\hbar\omega > E_g$ is discussed below. However, on the other hand, there is a fundamental similarity in the behavior of the systems under consideration. It manifests itself in the fact that PL attributable to manganese and its excitation in $Zn_{0.995}Mn_{0.005}S$ and $Zn_{0.99}Mn_{0.01}O$ occur via a series of localized states coupled between themselves. For $Zn_{0.995}Mn_{0.005}S$ at $\hbar\omega < E_g$, this is the series of intracenter states of the d^5 shell of Mn^{2+}. For $Zn_{0.99}Mn_{0.01}O$ at $\hbar\omega > E_g$, this is the series of localized states in the valence band that appear due to strong d–p-hybridization (Fig. 4).

Strong hybridization of the $3d$-states of Mn^{2+} and the $2p$-states of the ions of the immediate environment in $Zn_{1-x}Mn_xO$ is attributable to a smaller cation–anion separation in ZnO than that in ZnSe and ZnS. Dietl [7] put forward the idea that gallium nitride and zinc oxide doped with $3d$-impurities belong to the poorly studied class of dissolved magnetic semiconductors with strong hybridization. An increase in the degree of hybridization leads to an antiferromagnetic p–d-exchange interaction and hole localization on the ions of the close environment. A Zhang–Rice state introduced for the oxide superconductor La_2CuO_4 [8], which is characterized by hole localization on the $Mn^{2+}4O^{2-}$ cluster [7], emerges in the band gap of such compounds.

The existence of such a state was confirmed by calculations in the LSDA+U model [9]. The holes can be produced through the electron transport from the bond closest to Mn^{2+} into the conduction band. As a result, the hole is localized in the form of a Zhang–Rice-like state and a wide band of intense absorption emerges. Thus, Dietl [7] explained the strong absorption in $Zn_{1-x}Mn_xO$ in the range (2.2–3) eV that cannot be understood as the result of intracenter transitions commonly observed in $Zn_{1-x}Mn_xSe$ and $Zn_{1-x}Mn_xS$ in this range or as transitions with charge transfer, because Mn^{2+} in ZnO have no donor d^5/d^4 or acceptor d^5/d^6 levels in the band gap [10]. Thus, the absorption bands can serve as a way of detecting Zhang–Rice states. However, the Zhang–Rice-like state in the PL spectrum does not manifest itself as a band shifted toward lower energies relative to the edge of the absorption band, like the PL band in $Zn_{1-x}Mn_xSe$ and $Zn_{1-x}Mn_xS$ due to the transition ($^4T_1$–$^6A_1$). This is explained by a nonradiative transition whose mechanism is not yet clear [11].

In [7], the strong bonding condition is expressed as the ratio of the impurity potential U to the critical value of U_c at which a bound state is formed, $U/U_c > 1$. In this case, a bound Zhang–Rice-like state emerges and a positive addition to the change in band gap $E_g(x)$ appears. If $U/U_c < 1$, then the addition is negative and $E_g(x)$ decreases at low x, as is observed for

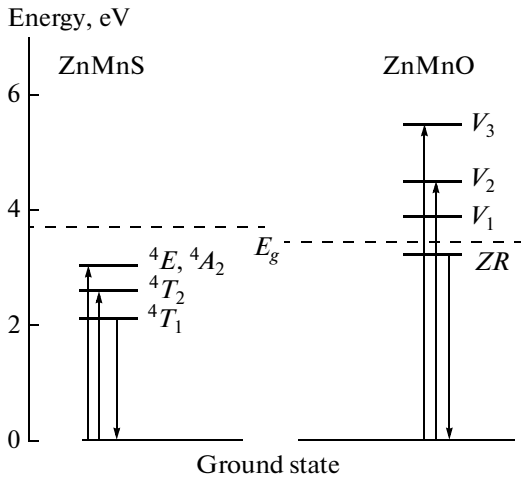

Fig. 4. Left: the energy level diagram for Mn^{2+} in a $Zn_{1-x}Mn_xS$ single crystal; the $^4T_1$–$^6A_1$ transitions forming the 2.12 eV luminescence band and the transitions to higher intracenter states that form the peaks in the PLE spectrum are shown. Right: the diagram of localized states for a $Zn_{1-x}Mn_xO$ compound; the transitions forming the 2.9-eV PL peak (ZR) and peaks V_2 and V_3 in the PLE spectrum are shown.

$Zn_{1-x}Mn_xSe$ [12]. In our experiment for nanopowders, the energy lines of the free excitons coupled to the two upper inverted [6] valence subbands Γ_7 and Γ_9 and the exciton coupled to the third, lower valence subband Γ_7 shift upward by 7 and 12 meV, respectively, which clearly indicates that $E_g(x)$ increases. Therefore, we can confidently consider the condition for strong bonding between the Mn^{2+} spin and the hole on the nearest oxygen ions in $Zn_{1-x}Mn_xO$ to be satisfied [7].

Given the above reasoning, the bands V_1–V_3 in the PLE spectrum of the 2.9 eV peak could be associated with the states that appear due to strong hybridization deep in the valence band. However, the decrease in the intensity of the 2.9 eV PL peak we revealed and the weakening of the excitation spectrum of this emission in $Zn_{1-x}Mn_xO$ after annealing in air probably stem from the fact that the vacancies play a significant role in forming the 2.9 eV PL peak. It can be tentatively assumed that PL is also produced by the $Mn^{2+}4O^{2-}$ cluster whose close environment includes an oxygen vacancy, for example, in the second oxygen coordination sphere. In this case, strong hybridization of the *d*-states with the *p*-states of the nearest O^{2+} ions will also take place and this gives us grounds to believe that the energy of the Zhang–Rice-like state will most likely be different. The shallow state through which the emission with the 2.9 eV peak occurs is "pushed out" into the band gap, i.e., the vacancy somehow activates radiative recombination via the state that appears due to strong *d*–*p*-hybridization. The wide bands of distorted states appear due to the same hybridization in the valence band. It seems natural that there exists a commonality between the hybridization-distorted states of the valence band and the Zhang–Rice-like state pushed out into the band gap, because both are formed in the region of the crystal around the Mn^{2+} ions. This manifests itself in the PLE spectrum as the bands V_1, V_2, and V_3 at energies of 3.9, 4.5, and 5.3 eV. It is these states that are shown in Fig. 4. The rise in the excitation spectrum of the 2.9 eV peak can be understood as follows. The hole appearing at $\hbar\omega > E_g$ rapidly loses its energy, moving over the energy states in spatially bounded regions around the Mn^{2+} ions and falls into a localized Zhang–Rice-like state, with the immediate environment of Mn^{2+} being charged positively. Therefore, the electron falls to a hydrogen-like orbit and recombines radiatively with a higher probability than that of nonradiative annihilation in the surface layers. The number of such radiative recombinations is determined by the density of the hybridization-distorted states. Thus, we obtain a method for investigating these states deep in the valence band. Note that the bands V_1, V_2, and V_3 manifest themselves in a very weak form on the descent of the excitation spectrum of the 2.1-eV peak in $Zn_{1-x}Mn_xO$ nanopowders (Fig. 1b, curve *2*). This is possible if the deep impurity center through which the 2.1-eV emission occurs is located near Mn^{2+}.

Thus, we found that the intensities of the 2.9 eV peak in the PL spectrum and the 3.9, 4.5, and 5.3 eV peaks in the excitation spectrum of the 2.9-eV emission for $Zn_{1-x}Mn_xO$ nanocrystals [4] decrease with reducing number of oxygen vacancies. This provides further evidence for an important role of the oxygen vacancies in forming the properties of oxide materials. We provided qualitative considerations that the 2.9-eV peak in the PL spectrum and the bands V_1, V_2, and V_3 in the excitation spectrum of the 2.9-eV emission result from strong hybridization in the $Zn_{1-x}Mn_xO$ system [7, 9]. Strong hybridization in $Zn_{1-x}Mn_xO$ is confirmed by an increase in the band gap for low values of *x*. On the whole, the origin of the 2.9-eV peak and notably the shape of its excitation spectrum are as unexpected for $Zn_{1-x}Mn_xO$ as the intense absorption in the range (2.2–3) eV and require further studies.

ACKNOWLEDGMENTS

We wish to thank T. Dietl, V.I. Anisimov, and A.V. Lukoyanov for the discussion of localized states in the $Zn_{1-x}Mn_xO$ system. This work was supported by the Russian Foundation for Basic Research (project nos. 07-02-00910_a and 08-02-99080r-ofi), and Russian Federal Agency on Science and Innovations (grant no. 02.740.11.0217).

REFERENCES

1. B. K. Roberts, A. B. Pakhomov, P. Voll, and K. M. Krishnan, Appl. Phys. Lett. **92**, 162 511 (2008).

2. K. Kikoin and V. Fleurov, Phys. Rev. B: Condens. Matter **74**, 174407 (2006).

3. A. Sandaresan, R. Bhargavi, N. Rangarajan, U. Siddesh, and C. N. R. Rao, Phys. Rev. B: Condens. Matter **74**, 161306 (2006).

4. V. I. Sokolov, A. Ye. Yermakov, M. A. Uimin, A. A. Mysik, V. A. Pustovarov, M. V. Chukichev, and N. B. Gruzdev, J. Lumin. **129**, 1771 (2009).

5. V. I. Sokolov, A. E. Yermakov, M. A. Uimin, A. A. Mysik, V. B. Vykhodets, T. E. Kurennykh, V. S. Gaviko, N. N. Shchegoleva, and N. B. Gruzdev, Zh. Éksp. Teor. Fiz. **132** (1), 77 (2007) [JETP **105** (1), 65 (2007)].

6. I. P. Kuz'mina and V. A. Nikitenko, *Zinc Oxide: Preparation and Optical Properties* (Nauka, Moscow, 1984), p. 111 [in Russian].

7. T. Dietl, Phys. Rev. B: Condens. Matter **77**, 085 208 (2008).

8. F. C. Zhang and T. M. Rice, Phys. Rev. B: Condens. Matter **37**, 3759 (1988).

9. T. Chanier, F. Virot, and R. Hayn, Phys. Rev. B: Condens. Matter **79**, 205 204 (2009).

10. K. A. Kikoin and V. N. Fleurov, *Transition Metal Impurities in Semiconductors: Electronic Structure and Physical Properties* (World Scientific, Singapore, 1994), p. 86.

11. R. Beaulac, P. I. Archer, and D. R. Gamelin, J. Solid State Chem. **181**, 1582 (2008).

12. R. B. Bylsma, W. M. Becker, J. Kossut, U. Debska, and D. Yoder-Short, Phys. Rev. B: Condens. Matter **33**, 8207 (1986).

Translated by V. Astakhov